

Implications of Shifting Stratification Dynamics on Phytoplankton Blooms in San Francisco Bay Under Future Scenarios

Emma Nuss, Dave Senn, Derek Roberts, others?

Keywords:

1. Introduction

Eutrophication frequently occurs in estuarine and shallow coastal environments where an excess of nutrients runoff, fueling increased algal growth, and leading to low dissolved oxygen levels. San Francisco Bay (SFB) is an urbanized estuary with high nutrient loads from agricultural and stormwater runoff and wastewater treatment plant (WWTP) discharge. Wastewater discharge provides the largest proportion (65%) of nutrient loads to the estuary, with runoff from agriculture via the Sacramento-San Joaquin River Delta making up 20% and local storm-water runoff making up 15% (SFEI 2014 Nutrient Loading Study**). Despite these high nutrient loads and high ambient nutrient concentrations within SFB, spring chlorophyll blooms are not consistently large and have strong inter-annual variability (cite**).

Previous work has shown that high turbidity and benthic grazers can exhibit controls on phytoplankton growth (cite**). For example, in the north part of SFB, an invasive clam species (*Corbicula fluminea*) strongly modulates phytoplankton biomass (cite** Lucas et al 2002; Lopez et al. 2006). Additionally, throughout the Bay, suspended sediment concentrations can

18 limit light availability, inhibiting phytoplankton growth. The photic zone in
19 San Francisco Bay is typically ** meters, but varies over numerous timescales
20 (cite**).

21 The effect of suspended sediment and benthic grazers are both modulated
22 by the strength of stratification of the water column. Stronger stratification
23 allows phytoplankton to spend more time in the upper part of the water
24 column, increasing the light levels they experience and their distance from
25 benthic grazers. Phytoplankton blooms in South SFB have been observed
26 to be associated with stratification (Cloern 1991**). Stratification in tidal
27 estuarine environments are controlled by horizontal salinity gradients set up
28 through freshwater flows to the estuary. The salinity gradient and the effect
29 of tides on this gradient can create periodic stratification known as strain-
30 induced periodic stratification (SIPS) (cite**). When the salinity gradient
31 is strong enough and tidal mixing is weak enough, SIPS can set up vertical
32 stratification which can persist through multiple tidal cycles, given the right
33 conditions. Stratification that persists through multiple tidal cycles provides
34 phytoplankton ideal growth conditions. Prolonged stratification decreases
35 the depth of the mixed layer and ensures that phytoplankton are exposed to
36 higher light levels.

37 While stratification has been shown to be an important control on phy-
38 toplankton growth in SFB, the relationship has not been fully quantified
39 and the relationship between stratification and phytoplankton growth is not
40 predictive. Northern California precipitation projections predict increases in
41 extreme wet and dry years, as well as increases in sub-seasonal storms (Swain
42 et al **). This change in precipitation patterns will affect the distribution

43 of salinity in SFB and, in turn, stratification dynamics. Quantifying the re-
44 lationship between stratification and chlorophyll and developing predictive
45 capability would be instrumental in understanding future ecological condi-
46 tions in SFB and assist in making management decisions that would affect
47 the health of the bay.

48 In this study we focus on South SFB, which exhibits the highest am-
49 bient nutrient concentrations (SFEI 2014 Nutrient Loading Study**). In
50 addition to high nutrient concentrations, this subembayment has longer res-
51 idence times than any other part of the bay. High nutrient concentrations,
52 in conjunction with long residence times, provide a system that could be
53 susceptible to low dissolved oxygen concentrations and poor ecological con-
54 ditions. We aim to understand South SFB's susceptibility to eutrophication
55 conditions under changes in freshwater flow and shifts in stratification dy-
56 namics.

57 This study makes use of the long-term water quality dataset collected by
58 USGS along the transect of SFB and a hydrodynamic model developed for
59 SFB. It is hypothesized that sustained stratification events could lead to in-
60 creased chlorophyll levels. We aim to quantify the importance of stratification
61 in observed chlorophyll using this long-term dataset and use a probabilistic
62 approach to estimate a relationship. We use this relationship and the hydro-
63 dynamic model to predict the effect of various freshwater flow conditions on
64 chlorophyll conditions in South SFB, and how these could act as proxies for
65 future climate scenarios.

2. Methods

2.1. Data

Data sets of South Bay salinity, stratification, tidal velocity, freshwater flow, and chlorophyll were compiled and used to understand the effect of environmental conditions on chlorophyll observations. United States Geological Survey (USGS) Alameda Creek (USGS Station 11179000) daily flow data was used for an estimate of South Bay freshwater flow conditions. National Oceanic and Atmospheric Administration (NOAA) acoustic doppler current profiler (ADCP) data at San Mateo Bridge was harmonically decomposed and used to create tidal velocity predictions for the desired time record. Salinity and chlorophyll data from USGS bi-monthly cruises were compiled for South Bay stations (22 - 32).

To quantify the relationship between chlorophyll and environmental conditions, we utilize the data to complete a conditional probabilistic analysis of the likelihood of chlorophyll given various conditions. This analysis required data to be on a synchronous time interval. Raw data was available on a number of different timescales, from bi-monthly to sub-daily, and as such, different mechanisms were used to create daily records. Tidal velocity data was sub-sampled from hourly to daily by extracting the daily maximum flood velocity. Depth averaged salinity data at South Bay stations were interpolated through time using a generalized additive model (details from Dave). This interpolated salinity data was used to calculate daily horizontal salinity gradient metrics. Raw salinity data was used to calculate stratification only for the days available and was left masked on days with no data. Similarly, chlorophyll data was kept as raw data for available days and

91 freshwater flow data already was given as daily flow. The final version of
 92 this processed data set included daily maximum flood velocity at San Mateo
 93 Bridge, daily interpolated longitudinal salinity gradient between South Bay
 94 USGS cruise stations (22-32), daily flow at Alameda Creek, and stratifica-
 95 tion and chlorophyll at South Bay USGS cruise stations (22-32) for available
 96 days.

The horizontal Richardson number (Ri_x) was calculated from daily salin-
 ity gradient and tidal velocity data as a vertical stratification metric. Ri_x
 is a metric that captures the balance between the stratifying forces of tidal
 straining and the destratifying forces of tidal mixing and is defined as:

$$Ri_x = \frac{\beta g \frac{ds}{dx} H^2}{u_*^2} \quad (1)$$

97 where $\frac{ds}{dx}$ is the horizontal salinity gradient, H is the water depth, g is gravity,
 98 β is the saline contraction coefficient, and u_* is the friction velocity. Ri_x was
 99 calculated for each day in the data range using mean water depth, 10% of
 100 the daily maximum flood velocity as an approximation for friction velocity
 101 ($u_* = 0.1u_{tidal}$), and the depth-averaged horizontal salinity gradient between
 102 USGS station 27 and 32.

103 2.2. Probabilistic Analysis

104 A probabilistic approach was taken to analyze the data. The calculated
 105 Ri_x and observed chlorophyll was used to calculate pseudo-conditional prob-
 106 ability distributions of the likelihood of observing chlorophyll for a given Ri_x .
 107 To do this, we first applied a 3-day backwards-looking window to the daily
 108 Ri_x and selected the minimum value in that window to produce a minimum
 109 Ri_x time series. Next, quantile ranges were chosen to apply to Ri_x , binning

110 the coinciding observations into each respective quantile range. For each Ri_x
 111 quantile range, the coincident chlorophyll data points were subset. From this,
 112 the chlorophyll observations were further subdivided into chlorophyll quan-
 113 tile ranges. The probability of observing chlorophyll of a given quantile or
 114 higher was calculated from the subset of chlorophyll data by computing the
 115 frequency of observations in which the subset of chlorophyll observations ex-
 116 ceeded the quantile range threshold and then divided by the total number of
 117 observations of the subset of chlorophyll. This process was repeated for each
 118 Ri_x quantile chlorophyll quantile pair, creating a 2-dimensional probability
 119 map.

These probability calculations result in gridded data of the probability of
 observing chlorophyll above a chosen chlorophyll quantile, given a minimum
 quantile of Ri_x in the 3 days prior to the observation. This gridded data
 can be converted to a continuous function, which can be used to estimate
 the probability of exceeding a given chlorophyll quantile for any given Ri_x
 quantile. This continuous function is achieved through the use of radial basis
 functions. The general form of a radial basis function is:

$$s(\vec{x}) = \sum \alpha_i \Phi_i(|\vec{x} - \vec{x}_i|), \quad (2)$$

where α_i are weights (estimated through least squares), Φ_i are the basis
 functions, \vec{x} is the coordinate location (i.e., the given chlorophyll and Ri_x
 pairs), and \vec{x}_i are the reference locations of known values. The chosen form
 of the basis function is a polyharmonic spline of the form:

$$\Phi(r) = r^2 \ln(r). \quad (3)$$

For our setup, $r = \vec{x} - \vec{x}_i$, indicating that the radial distance is measured as

the distance from given chlorophyll (q_{chl}) and Ri_x quantiles (q_{Ri_x}) from the reference quantiles used in the probability calculations from observations:

$$r(q_{chl}, q_{Ri_x}) = \sqrt{(q_{chl} - q_{chl}(i))^2 + (q_{Ri_x} - q_{Ri_x}(i))^2} \quad (4)$$

The result is a function ($s(q_{chl}, q_{Ri_x})$) that calculates probability given a choice of chlorophyll quantile threshold (q_{chl}) and a Ri_x quantile (q_{Ri_x}):

$$s(q_{chl}, q_{Ri_x}) = \sum \alpha_i \Phi_i(r(q_{chl}, q_{Ri_x})). \quad (5)$$

120 2.3. Hydrodynamic Model

121 To explore realistic hydrodynamic conditions under various freshwater
 122 flow conditions we utilize a hydrodynamic model that is set up and calibrated
 123 for SFB. The hydrodynamic model is built on *D-Flow Flexible Mesh* (DFM), a
 124 finite-volume, three-dimensional, unstructured hydrodynamic model (Martyr-
 125 Koller et al 2017**). The original model setup was developed and outlined
 126 in Pubben 2017** as a part of the USGS Computational Assessments of Sce-
 127 narios of Change for the Delta Ecosystem (CASCaDE) and San Francisco
 128 Bay-Delta Community Model projects. The most pertinent model details are
 129 given below; however, a full description of hydrodynamic model setup and
 130 validation of performance can be found in the San Francisco Bay Interim
 131 Model Validation Report **cite**.

132 2.3.1. Model Grid

133 The model is an unstructured horizontal grid with sigma vertical levels.
 134 The model grid encompasses SFB and extends into the coastal ocean, from
 135 approximately 20 km off of Point Reyes in the north-west corner and 40 km
 136 west of Half Moon Bay in the southwest corner, roughly covering the San

137 Francisco Bight (Fig. 1). Horizontal grid resolution varies from fine scale
 138 resolution (20 m) in shallow slough areas to over 2 km in the offshore, for a
 139 total of 49,996 grid cells. Nominal resolution for areas of interest are between
 140 250 m (South SFB) and 350 - 500 m (North SFB). In the vertical, there are
 141 10 sigma layers, with varying layer thickness in relation to water depth.

142 Bathymetry is prescribed at the nodes of each grid cell from linear in-
 143 terpolation of 10 m topo-bathymetry from California Department of Wa-
 144 ter Resources (Wang and Ateljevich, 2012***) and high-resolution USGS
 145 bathymetry in Lower South Bay (Foxgrover et al, 2014***). Elevation data
 146 are relative to the NAVD88 vertical datum.

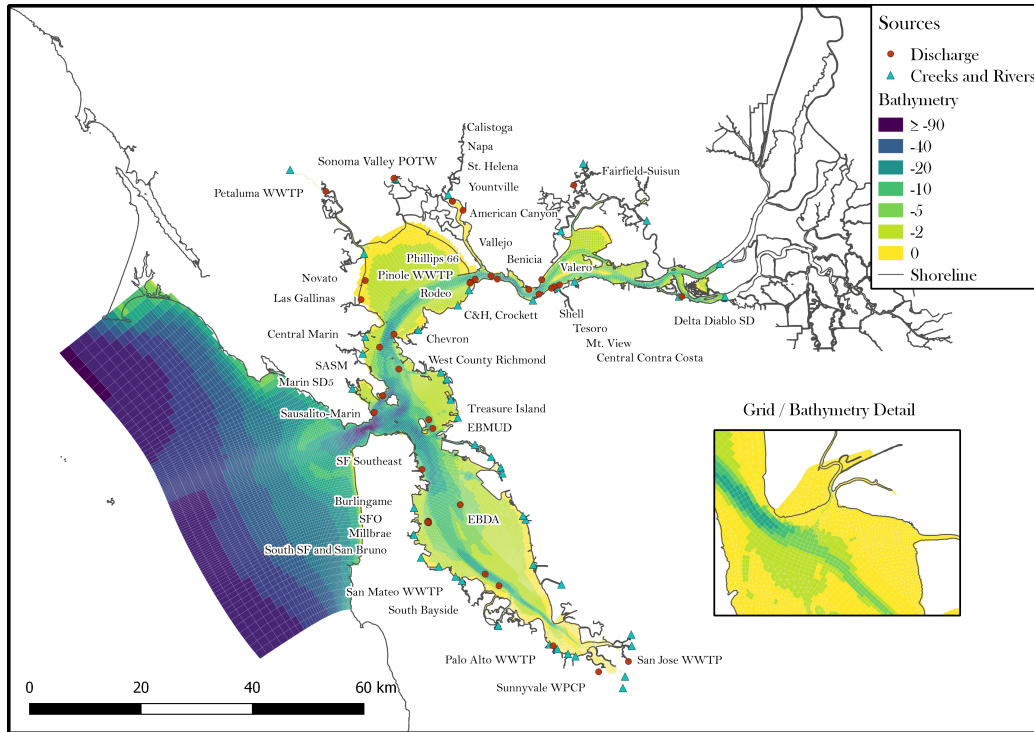


Figure 1: San Francisco Bay DFM grid

147 2.3.2. Boundary Conditions

148 The open ocean boundary is tidally forced with observed 6-minute water
149 level data (NOAA gage 9415020) and salinity and temperature are set to
150 33 ppt and *** respectively. Water level forcing data is low-pass filtered
151 with a 4th-order Butterworth filter with a 3-hour cutoff period. The shorter
152 northern and southern edges of the ocean boundary are closed.

153 Freshwater flows were derived from the Bay Area Hydrologic Model (a
154 HSPF-based hydrologic model**cite?), calibrated against gage data over the
155 2000–2016 period. This model includes ***check this number*** 44 separate
156 river and stormwater inputs to SFB (Fig. 1). All river and stormwater inputs
157 are assumed to enter the Bay with negligible salinity (i.e. 0 ppt) and constant
158 temperature of 20°C.

159 The edge of the model domain is at Rio Vista on the Sacramento River,
160 and Jersey Point on the San Joaquin River. Boundary conditions here are
161 taken from USGS streamflow gages (11455420 and 11337190 for the Sacra-
162 mento and San Joaquin flows, respectively). Salinity is negligible and set
163 accordingly, while water temperature is obtained from the same USGS gag-
164 ing stations and assigned to in-flowing water in the model.

165 Wastewater treatment plants (WWTPs) inputs can be significant fresh-
166 water sources and influence the density field. Flow and load data for 37
167 WWTPs and 5 refineries are used as inflows to the bay. For dates when flow
168 data is unavailable, a flow rate is estimated based on inter-annual trends and
169 a seasonal flow climatology. Each of the 42 inflows have been added to the
170 hydrodynamic model as a freshwater source located at the bed.

171 The wind field is interpolated from 52 wind stations around SFB and

172 specified hourly on a 1.5 km by 1.5 km grid. Specifics of the interpolation
173 method and data sources can be found in King (2019) ****cite****.

174 In addition to stormwater runoff, which enters the model at prescribed
175 locations along the boundary, we also include direct precipitation and evapo-
176 ration acting directly on the water surface. The model incorporates measured
177 precipitation and evapotranspiration (ET°) from the CIMIS Union City sta-
178 tion.

179 **3. Results**

180 *3.1. Probabilistic Analysis*

181 Our probabilistic analysis relies heavily on the calculated stratification
182 metric, Ri_x . This metric is compared to the cruise-averaged stratification
183 profiles from USGS stations 24, 25, 27, and 29. Multiple stations were aver-
184 aged together to minimize noise from any one station’s variability and also to
185 compare how Ri_x captures the aggregate stratification condition in this re-
186 gion of the bay. USGS cruises sample at various phases in the tidal cycle and
187 thus the observed stratification may at times be biased by ebb tide stratifi-
188 cation due to tidal straining; however, Ri_x tends to agree well with observed
189 stratification (Fig. 2). Times of observed strong stratification correspond
190 well with higher Ri_x .

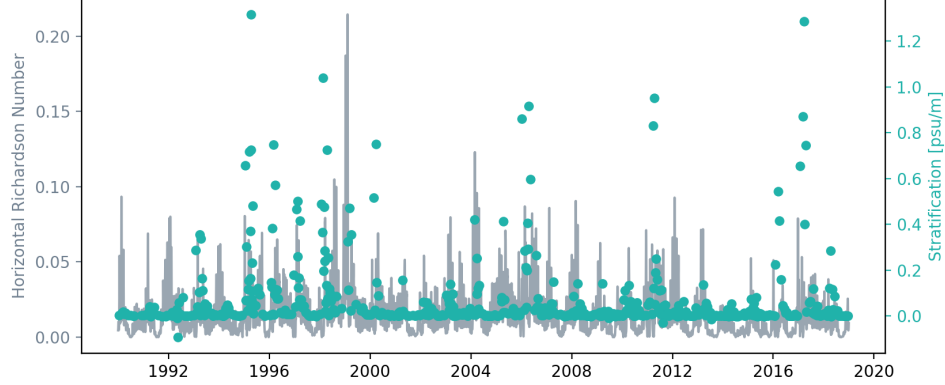


Figure 2: Calculated daily horizontal Richardson number and observed stratification averaged between USGS stations 24, 25, 27, and 29

191 Ten quantile bins evenly spaced between 0 and 1 were defined for Ri_x in
 192 bin sizes of 0.1. Chlorophyll observations were subset by the corresponding
 193 3-day windowed Ri_x . The number of observations (n-value) for each chloro-
 194 phyll subset hovered around 55 for each Ri_x quantile bin. The probability
 195 of observing chlorophyll at greater than or equal to a particular chlorophyll
 196 threshold was calculated for each chlorophyll subset using varying chlorophyll
 197 quantile thresholds from 0.1 to 0.9. The contours in Figure 3 show the results
 198 of these calculations. The probability of observing a chlorophyll level of 0.1
 199 quantile or higher is around 0.9-1.0 for all quantiles of Ri_x , indicating a very
 200 high likelihood that the chlorophyll level could exceed this very low thresh-
 201 old. Likewise, as the chlorophyll threshold is increased in the probability
 202 calculation, probabilities drop rapidly resulting in their minimum values at
 203 the highest chlorophyll threshold (quantile 0.9) ranging from approximately
 204 0 to 0.18 the Ri_x quantile increases. Probabilities generally increase as you

205 increase Ri_x and decrease as you increase chlorophyll quantile. These re-
 206 sults support the hypothesis that more stratification can lead to increased
 207 likelihood of high chlorophyll levels.

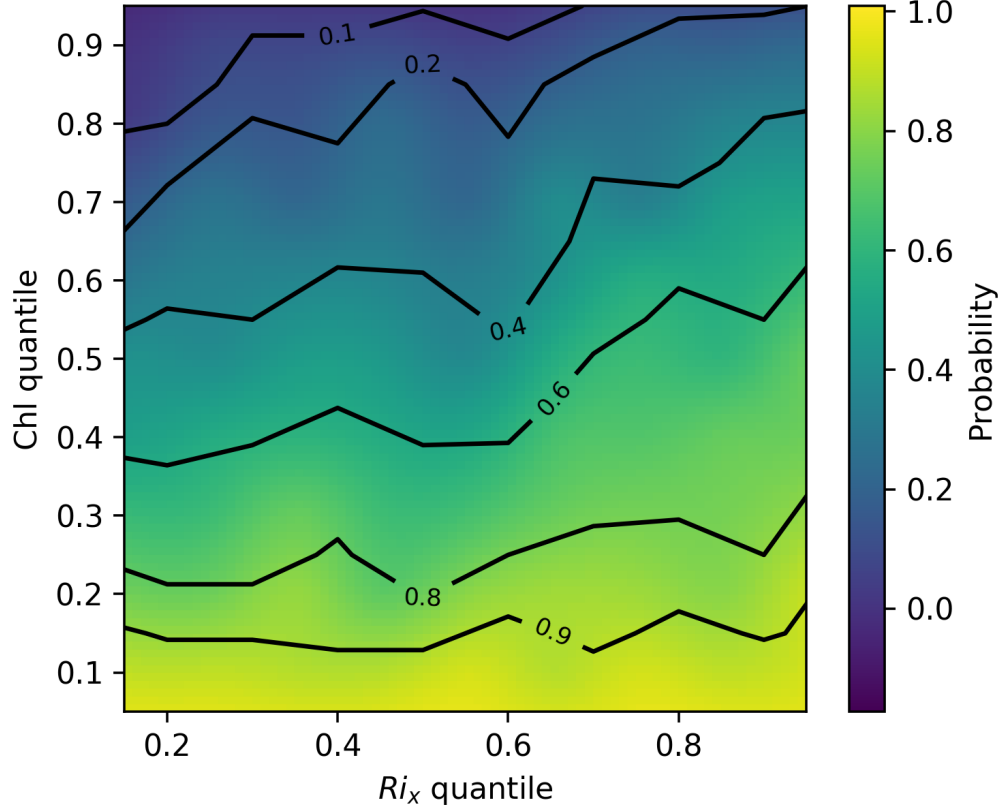


Figure 3: Probability of observing chlorophyll of the corresponding chlorophyll quantile or higher given the observed Ri_x quantile in the 3 days prior. Contours indicate the results directly from observations. Shading displays these same calculated probabilities, but calculated with equation 5 for finer resolution.

208 Equation 5 was used to create a continuous function from the calculated
 209 probabilities. The results are shown in Figure 3, where the contours show

the calculated probabilities directly from the data, while the shading shows the probabilities calculated via equation 5. Equation 5 captures the data well, and allows for calculation of probabilities for any set of chlorophyll and Ri_x quantiles. This capability is utilized with the model calculated Ri_X from hydrodynamic model output.

3.2. Hydrodynamic Simulation

The hydrodynamic model was run from August 2012 through September 2013 (Water Year 2013) and from August 2016 through September 2017 (Water Year 2017). For both runs, August through September were used as a two month spin up period. Validation of water level, velocity, temperature, and salinity for available locations and times provide good agreement. A detailed validation of the model setup is found in ****(cite sfei validation report).

Water year 2013 and 2017 were chosen for simulation because the flow conditions observed in both years served as observational extremes. Water year 2013 was a low flow year in the midst of a state-wide drought. Conversely, 2017 was an extremely wet year. These two years provide an interesting comparison of stratification conditions in San Francisco Bay and provide proxies for projected future conditions.

To analyze the model output, Ri_x was calculated in a similar manner as the observations used the probabilistic analysis. Ri_x was calculated as the distance normalized salinity difference between the approximate locations of San Mateo Bridge and Dumbarton Bridge in the model grid. This horizontal salinity gradient data was down-sampled to daily data by taking the average over each day. Depth-averaged tidal velocity data was taken at San Ma-

235 teo Bridge and down-sampled to daily data by taking the daily maximum
236 flood velocity. Water depth data was taken at San Mateo Bridge and down-
237 sampled to daily data by taking the day average water depth. The daily
238 Ri_x was calculated from the modeled data by the same method described in
239 Section 2.1.

240 Distributions of Ri_x from observations, water year 2013, and water year
241 2017 are compared in Figure 4. The following statistical calculations are
242 performed for a log distribution. The distribution of observation calculated
243 Ri_x has a mean of -2.0 and a standard deviation of 0.5. The range of the
244 observed distribution is from -4.9 to -1.0. The model calculated Ri_x for water
245 year 2013 has a mean of -2.2 and a standard deviation of 0.5. The range of
246 the water year 2013 distribution is -4.4 to -1.2. For water year 2017, the
247 mean is -1.8 and the standard deviation is 0.4. The range of the distribution
248 is from -3.3 to -0.6. These distributions match with expectations, where
249 the observed Ri_x distribution is relatively log normally distributed spanning
250 roughly the same range as both water year 2013 and 2017. The distribution
251 of water year 2017, an extreme wet year, is shifted towards stronger Ri_x as
252 would be expected and conversely water year 2013 is shifted towards weaker
253 Ri_x .

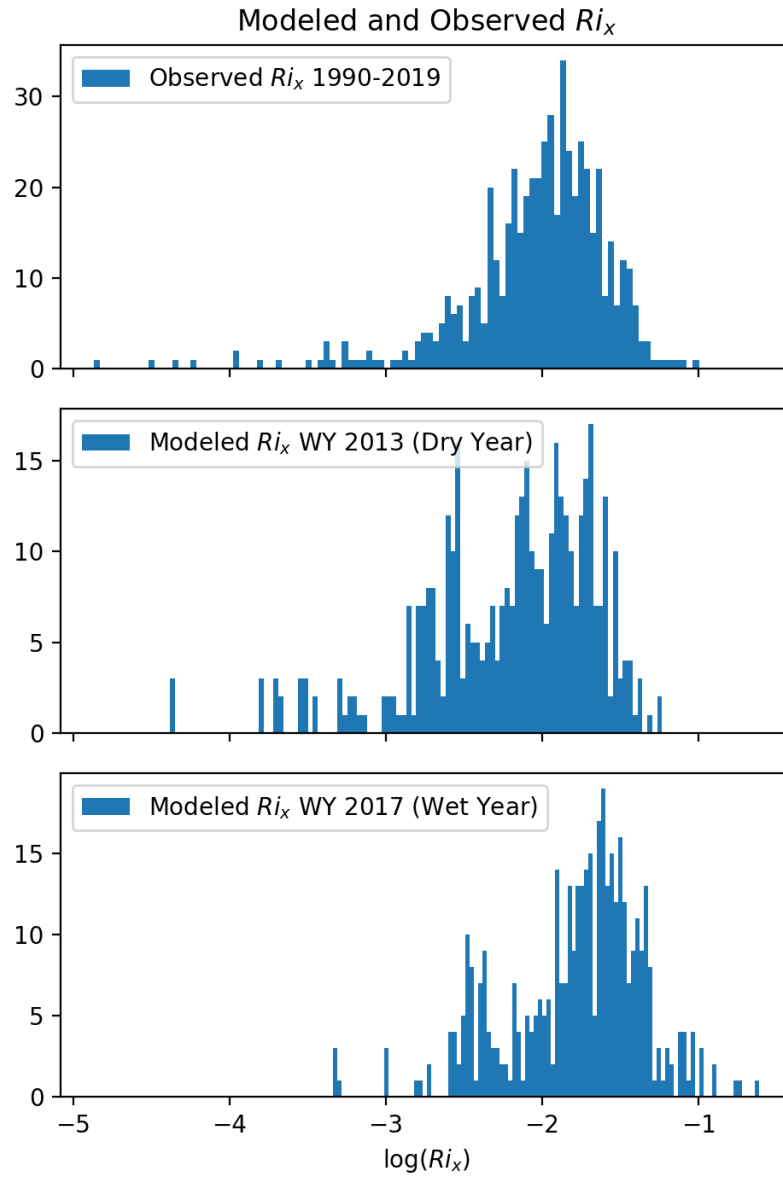


Figure 4: Histograms of daily 3-day windowed Ri_x , as calculated from observations, water year 2013 model output, and water year 2017 model output.

254 To use equation 5 with the model conditions, the model calculated Ri_x
 255 are converted to an equivalent quantile from within the observation calcu-
 256 lated distribution. Figure 5 shows the distribution of the quantiles for both
 257 model years and observations. As expected, observation quantiles are evenly
 258 distributed between 0 and 1; however, the histograms of water year 2013
 259 and 2017 show different distributions. Water year 2013 has a higher fre-
 260 quency of low quantiles, whereas, water year 2017 has a high frequency of
 261 high quantiles (Fig. 5). These quantile distributions are consistent with the
 262 Ri_x distribution statistics and the conditions observed in each year.

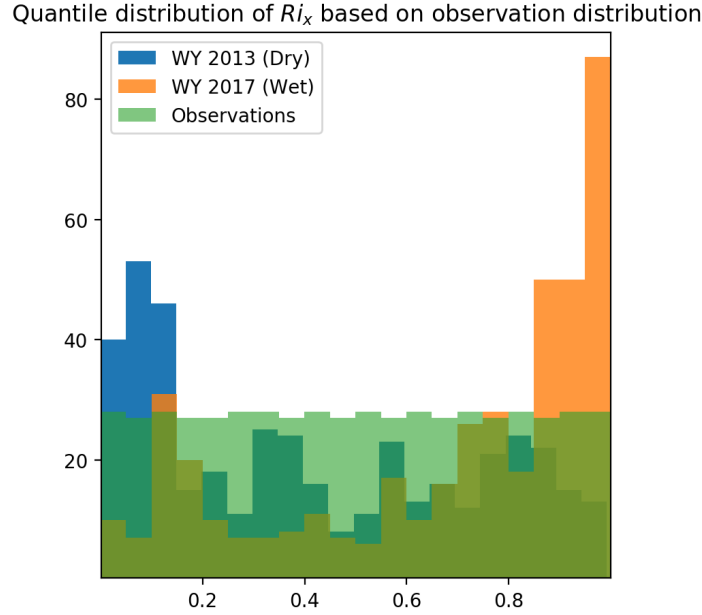


Figure 5: Histogram of number of Ri_x values in each quantile of the observation calculated distribution of Ri_x . Green bars indicate the observation Ri_x distribution, as seen by being nearly evenly distributed across all quantiles. Water year 2013 is indicated by the blue bars, and water year 2017 is indicated by the orange bars.

263 The Ri_x time series from both water year model runs were used to create
264 a time series of probabilities, using equation 5. Three chlorophyll quantile
265 thresholds (0.5, 0.75, 0.9) were used calculate this time series for each model
266 run. These quantile thresholds correspond to chlorophyll levels of 4.5, 6.9,
267 and 13.8 mg/m^3 .

268 Across all three chlorophyll thresholds, water year 2017 has a pattern of
269 more prolonged and higher probabilities of observing the given chlorophyll
270 quantile than water year 2013. Probabilities are highest, in both years, for
271 observing chlorophyll greater than the 0.5 quantile. Probabilities are more
272 consistently high through spring and into summer in water year 2017, whereas
273 water year 2013 probabilities drop significantly by June. If the probability
274 of exceeding a quantile (q) were a random variable, then the expected prob-
275 ability (p) is $p = 1 - q$. For example for a quantile of 0.75, the expected
276 probability is 0.25. Interestingly, in spring 2017, for all 0.5, 0.75 and 0.9
277 quantile thresholds, the probaility of observing those events given the Ri_x
278 conditions is increased above expected likelihood. There are periods in 2013
279 that exceed the expected likelihood as well, but are much fewer in frequency
280 and length.

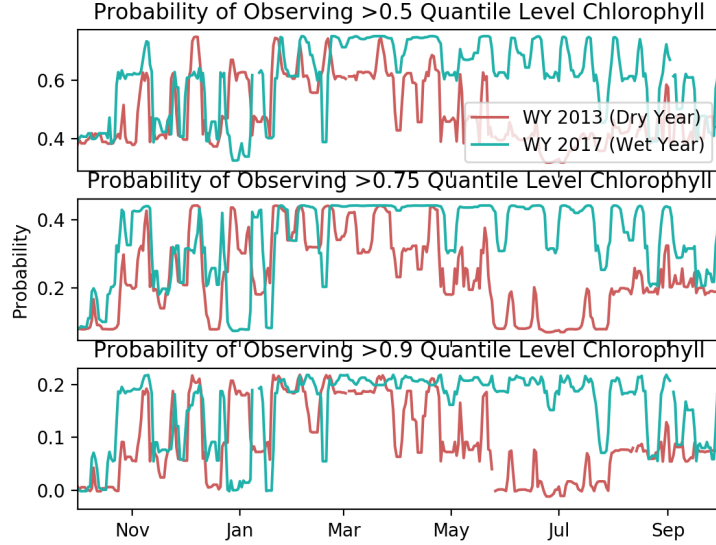


Figure 6: Probability of observing chlorophyll greater than the 0.5, 0.75, and 0.9 chlorophyll quantile, as calculated using the modeled daily 3-day windowed Ri_x for both water year 2013 and 2017.

281 The calculated probabilities correspond well with observed chlorophyll
 282 in South Bay. Average chlorophyll levels at South Bay USGS stations (24,
 283 25, 27, and 29) are shown with calculated probabilities in Figure 7. Ob-
 284 served chlorophyll levels exceed the 0.75 quantile threshold in spring 2017,
 285 which corresponds to a period of elevated probabilities. While spring 2013
 286 chlorophyll observations do not exceed the 0.75 quantile, they nonetheless
 287 are elevated, corresponding well with elevated probabilities; however, chloro-
 288 phyll levels are also elevated in July 2013 and probabilities are quite low
 289 and could be indicative of additional processes important to phytoplankton
 290 production.

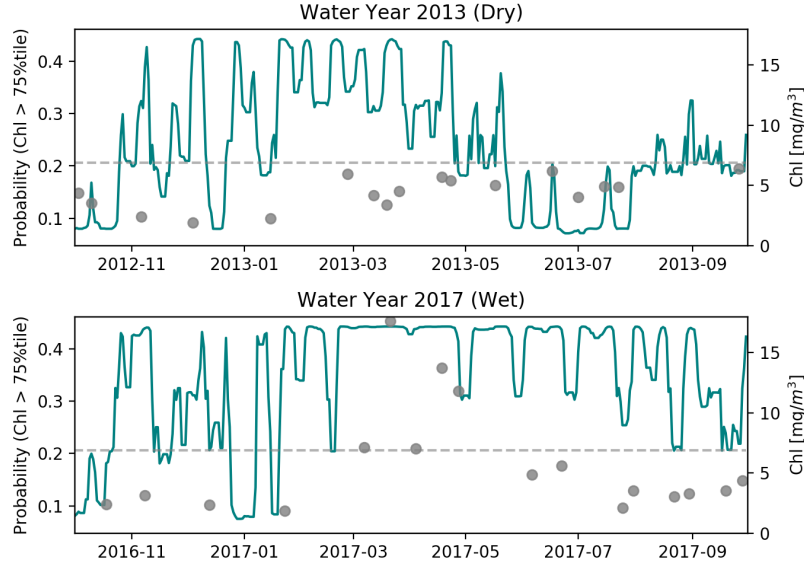


Figure 7: Comparison of the probability of observing chlorophyll greater than the 0.75 chlorophyll quantile, given the modeled daily 3-day windowed Ri_x for water year 2013 and 2017, and chlorophyll observations. Chlorophyll data is averaged between USGS stations 24, 25, 27, and 29 for each day data is available. The solid blue lines show the probability, given by the left hand axis. The grey dots indicate chlorophyll observations, given by the right hand axis. Water year 2013 is given by the top figure and water year 2017 is given by the bottom figure.

291 4. Discussion

292 The probabilistic method developed here is useful in its ability to utilize
 293 a relatively simple metric to calculate and predict the risk of phytoplankton
 294 blooms. It shows promise in successfully identifying periods of high likeli-
 295 hood of chlorophyll blooms which coincide with observed elevated levels of
 296 chlorophyll. While this method worked well identifying times during water
 297 year 2013 and 2017 when chlorophyll was elevated, work still needs to be done

298 to understand what constitutes a relevant elevated probability. For example,
 299 in spring 2017, the probability of observing chlorophyll above the 0.75 quan-
 300 tile threshold is elevated and persists around 0.4 for several months. During
 301 this time, there were multiple. During the same seasonal period in 2013,
 302 the probability is elevated but more variable and is not consistently as high.
 303 For this period, chlorophyll is slightly elevated, but does not exceed the 0.75
 304 quantile threshold. This difference suggests that sustained high probability
 305 periods matters in observing or that the relatively infrequent sampling could
 306 miss blooms events with shorter periods; however, more work needs to be
 307 done to make any conclusive conclusions.

308 The data used to develop the probabilistic relationship between chloro-
 309 phyll and Ri_x spanned 1990 - 2019. The 29 years of observations provide
 310 a large number of observations and visually provide a roughly log-normally
 311 distributed distribution of Ri_x (Fig. 4). Despite having a long time record,
 312 there is still a lack of information in the tails of the distribution. While this
 313 distribution is likely sufficient in capturing the relationship between Ri_x and
 314 chlorophyll within the time range of 1990 - 2019, using this distribution for
 315 future conditions may need some more work. Lack of data on the tails of the
 316 distribution may underestimate the extremes, which are of particular inter-
 317 est in projected future conditions. Also, while the observed Ri_x historically
 318 appears to be relatively stationary, future conditions could shift the mean
 319 Ri_x .

320 The core assumption of the probabilistic calculations and analysis is that
 321 stratification caused by SIPS is the dominant control on phytoplankton dy-
 322 namics. While there is evidence to support that this assumption is valid,

323 there are also other processes that may be important. The deep channel,
324 where the USGS data collected, is only a small portion of the entire bay.
325 Shallow shoals make up most of the bay by area. These shoals have different
326 dynamics due to their shallowness, and vertical stratification is much less sig-
327 nificant while suspended sediment concentrations driven by wind and wave
328 re-suspension are much more significant. These dynamics on the shoals can
329 occur separate to the channel stratification processes and elevated chloro-
330 phyll levels on the shoal may not coincide with ideal channel chlorophyll
331 conditions. In addition, mixing between the shoal and channel may play
332 a non-trivial input of chlorophyll to the channel. This method would not
333 capture these dynamics into predicting probabilities; however, this method
334 may aid in understanding historical events. Using this method to calculate
335 the likelihood of observing elevated chlorophyll conditions and comparing
336 to chlorophyll observations may aid in identifying times when chlorophyll
337 dynamics seem to fit within the stratification driven conceptual model and
338 when other dynamics, such as shoal-channel mixing, may be important.

339 While these results cannot be universally applied, some conclusions can
340 be drawn about the implications of shifting stratification dynamics on phy-
341 toplankton blooms in SFB. The differences in the calculated probabilities of
342 observing greater than the 0.75 and 0.9 quantiles of chlorophyll levels be-
343 tween 2013 and 2017 are striking (Fig. 6). In 2017, these probabilities are
344 elevated throughout the entire spring and summer, whereas the probabilities
345 are elevated for a brief period in spring 2013 and then drop significantly. This
346 difference, as well as observed chlorophyll levels, suggests that stratification
347 dynamics played a role in chlorophyll dynamics. The conditions of these two

348 years, particularly 2017, being proxies for projected extreme flow conditions
349 suggest that under future scenarios stratification favorable conditions and
350 subsequent phytoplankton blooms are likely expected.

351 5. Conclusions

352 This work successfully developed a method for quantifying the relation-
353 ship between chlorophyll and stratification dynamics by creating a proba-
354 bilistic function based on Ri_x . This probabilistic function allows for the
355 calculation of the conditional probability of observing chlorophyll exceeding
356 a specific quantile given the stratification conditions leading up to that ob-
357 servations. This method was applied to two years of hydrodynamic model
358 output, one serving as a dry year proxy and one serving as a wet year proxy.
359 Calculated probabilities captured the observed chlorophyll dynamics and in-
360 dicated strong differences between extreme wet and dry years, suggesting
361 that the likelihood of elevated chlorophyll levels will increase in extreme wet
362 years.

363 This method relies on several assumptions that limit the outcomes of
364 the results and future applicability of the method; the observed relation-
365 ship between Ri_x and chlorophyll observations is a stationary relationship,
366 and that stratification is the dominant control on phytoplankton dynamics.
367 These assumptions are reasonable for the purposes of the work presented in
368 this paper; however, there are some limitations and issues to carefully con-
369 sider in applying this method to other scenarios. Future work could explore
370 more fully how stratification conditions might change under future scenarios
371 through numerical modeling studies. In addition, more work needs to be

372 done to understand how important and when are other processes, such as
373 shoal-channel mixing, important in observed chlorophyll.

374 **References**